DOI: 10.1002/ejic.200600265

# Molecular Structures and NMR Studies of Lithium and Germanium(II) Complexes of a New Chelating Amido–Imino Ligand Obtained by Addition of *n*BuLi to 1,2-Bis(arylimino)acenaphthene

**Igor L. Fedushkin,*[a] Markus Hummert,[b] and Herbert Schumann[b]**

*Dedicated to Prof. Vladimir K. Cherkasov on the occasion of his 60th birthday*

**Keywords:** Lithium / N ligands / Germanium / Structure elucidation

The reaction of 1,2-bis[(2,6-diisopropylphenyl)imino]acenaphthene (dpp-bian, **1**) with 1 equiv. of *n*BuLi in diethyl ether or with 2 equiv. of *n*BuLi in hexane produces [{dpp-bian(*n*Bu)}Li($Et_2O$)] (**3**) and [{dpp-bian(*n*Bu)Li}*n*BuLi]$_2$ (**4**), respectively. Complexes **3** and **4** are formed by the transfer of an *n*Bu anion to one of the imine carbon atoms of the dpp-bian ligand. Treatment of **3** and **4** with $H_2O$ affords the *C*-alkylated *N*-protonated amino-imino compound dpp-bian(H)(*n*Bu) (**5**). The reaction of **3** with $GeCl_2$(dioxane) affords the three-coordinate germylene complex [{dpp-bian(*n*Bu)}GeCl] (**6**). The molecular structures of **3**–**6** were determined by single-crystal X-ray structure analysis. The lack of symmetry in the alkylated bian system in **3**–**6** causes the non-equivalence of all protons except those of the $CH_3$ groups of the *i*Pr substituents.



## Introduction

In many respects, progress in organometallic and coordination chemistry is determined by the type of organic ligands used for the preparation of these metal complexes. The use of a new ligand system usually leads to complexes with more or less novel chemical properties. During the last decade, acenaphthene-1,2-diimines (bian) have become widely used as ligands in coordination chemistry. Diimine transition metal complexes serve as catalysts in alkyne hydrogenation,[1] C–C bond formation,[2] cycloisomerization,[3] hydrosilylation,[4] polymerization of alkenes[5] and acrylic monomers,[6] as well as in the copolymerization of $CO_2$[7] and $CH_2$=$CH_2$[8] with methylenecyclopropene, of ethylene with norbornene,[9] and of CO with styrene.[10] Thus, acenaphthene-1,2-dimine late transition metal complexes, the so-called Brookhart catalysts,[11] are some of the most effective catalysts for olefin polymerization known until now. The π-acceptor capability of the acenaphthene-1,2-dimine ligand causes an electron deficiency at the respective metal center that makes these complexes highly reactive towards organic substrates.

Recently, we have demonstrated for the first time that main group metals also readily form stable bian complexes. The most widely used ligand in this field is 1,2-bis[(2,6-diisopropylphenyl)imino]acenaphthene (dpp-bian, **1**). One of the remarkable features of the dpp-bian ligand in its main group metal complexes is its ability to adopt variable oxidation states. The reduction of dpp-bian with alkali metals in diethyl ether affords the mono-, di-, tri- and tetra-anions of the ligand, i.e. [(dpp-bian)$M_n(Et_2O)_m$] (M = Li, Na; $n$ = 1–4),[12] whereas with alkaline-earth metals the reduction of dpp-bian provides only dianions, forming the complexes [(dpp-bian)M$(THF)_n$] (M = Mg, Ca; $n$ = 2–4).[13] Depending on the reaction medium, the reduction of dpp-bian with aluminum in the presence of its halides gives the complexes [(dpp-bian)$AlCl_2$], [(dpp-bian)AlI($Et_2O$)], and [(dpp-bian)AlCl($Et_2O$)].[14] Alkylaluminum complexes with dpp-bian as a radical-anionic as well as a dianionic ligand are obtained by treating (dpp-bian)Na with $R_2AlX$ (R = Me, Et, *i*Bu; X = Cl, Br).[15] Similarly, the metal-exchange reactions of (dpp-bian)$Na_2$ or (dpp-bian)Na with $GeCl_2$ give the germanium(II) derivatives [(dpp-bian)Ge][16] and [(dpp-bian)-GeCl],[17] respectively. The variability of the oxidation state of the dpp-bian ligand is impressively demonstrated by the decomposition of [(dpp-bian)Mg(*i*Pr)($Et_2O$)], which occurs with elimination of *i*Pr radicals and simultaneous reduction of the dpp-bian radical anion to the dianion.[18] The oppo-

[a] G. A. Razuvaev Institute of Organometallic Chemistry of Russian Academy of Sciences,
Tropinina 49, 603950 Nizhny Novgorod, GSP-445, Russia
Fax: +7-8312-627497
E-mail: igorfed@imoc.sinn.ru
[b] Institut für Chemie der Technischen Universität Berlin,
Straße des 17. Juni 135, 10623 Berlin, Germany
Fax: +49-30-3142-2168
E-mail: schumann@chem.tu-berlin.de

   

site process, namely oxidation of the dpp-bian dianion to the radical anion, is observed in the reactions of [(dpp-bian)-$Mg(THF)_3$] (**2**) with organic substances such as aromatic ketones.[19] The course of the reactions of **2** with ethyl halides further demonstrates the non-innocence of the dpp-bian ligand in its metal complexes. They proceed by single-electron transfer from the dianionic dpp-bian ligand to EtX to yield an ethyl radical, which, in turn, attacks the ligand, which is now a radical anion, at one of the imino carbon atoms to give [(dpp-bian)(Et)MgX$(THF)_n$].[20] Acidic substances such as aliphatic ketones, terminal alkynes, and nitriles add to complex **2** with protonation of one of the ligand nitrogen atoms to produce complexes with unsymmetrical amido–imino dpp-bian ligands.[21] The different modes of the dpp-bian ligand (**A**: neutral; **B**: radical-anion; **C**: dianion) in the reactions of **2** with organic substrates, as well as the resulting modifications of the dpp-bian ligand (**D**: amino/imine and **E**: amido/amine), are shown below.

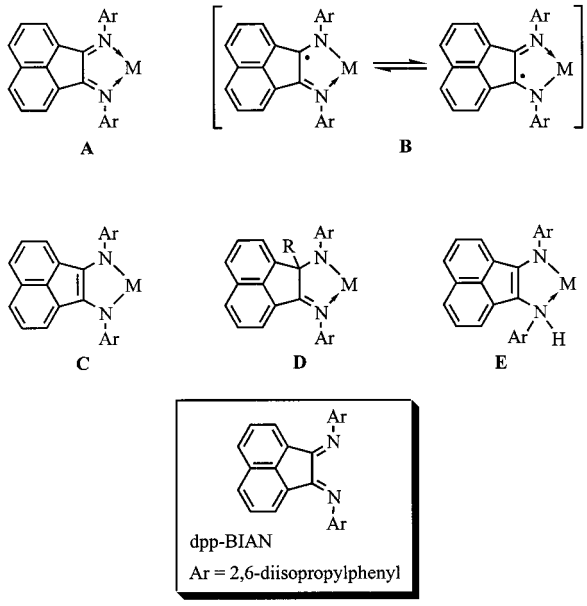


In this paper, we report on the alkylation of dpp-bian with *n*BuLi to provide the ligand system **D** and its subsequent reaction with $GeCl_2$.

## Results and Discussion

### Alkylation of dpp-bian with *n*BuLi

Addition of 1 equiv. of *n*BuLi to a suspension of dpp-bian in diethyl ether caused immediate dissolution of dpp-bian and a change in the color of the reaction mixture from yellow to blue. Crystallization of the foamy residue, remaining after removal of the solvents, from hexane afforded [dpp-bian(*n*Bu)]Li($Et_2O$) (**3**) in the form of blue, crystalline plates in 44% yield (Scheme 1).

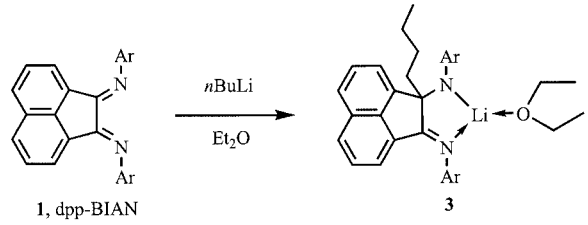


Scheme 1.

The reaction of equivalent amounts of dpp-bian and *n*BuLi also proceeded easily in hexane but produced yellow instead of blue crystals, the characterization of which by $^1H$ NMR spectroscopy in $C_6D_6$ is seriously hindered by multiple overlaps of the numerous signals. However, $[D_{10}]Et_2O$ solutions of both the blue and the yellow crystals give identical $^1H$ NMR spectra.

Addition of a twofold molar amount of *n*BuLi to a suspension of dpp-bian in hexane caused immediate precipitation of [{dpp-bian(*n*Bu)Li}*n*BuLi]$_2$ (**4**) as red crystals in 81% yield (Scheme 2).

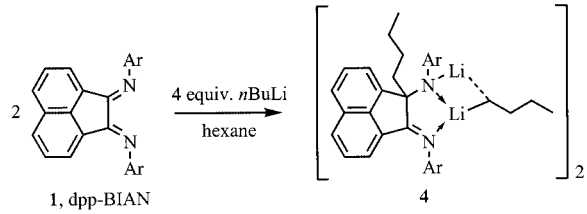


Scheme 2.

Hydrolysis of **3** and **4** resulted in the formation of the yellow, crystalline amino-imine [dpp-bian(H)(*n*Bu)] (**5**; Scheme 3).

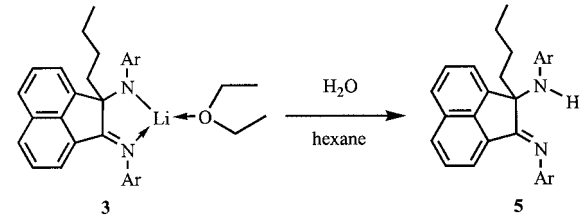


Scheme 3.

The anionic amido–imino ligand [dpp-bian(*n*Bu)]$^-$ of the lithium complex **3** can be transferred to other metal ions such as $Ge^{2+}$. Thus, the reaction of equimolar amounts of **3** and $GeCl_2$(dioxane) in $Et_2O$ afforded almost quantitative yields of red, crystalline [{dpp-bian(*n*Bu)}GeCl] (**6**), which contains three-coordinate $Ge^{II}$ (Scheme 4).

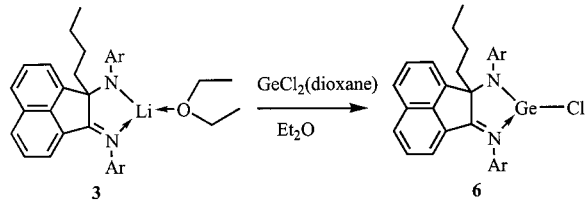


Scheme 4.

  

### Molecular Structures of Compounds 3–6

The molecular structures of **3**–**6** were determined by single-crystal X-ray analysis and are presented in the figures. Selected bond lengths and angles for **4**–**6** are presented in Tables 1 and 2, respectively. The low quality of the X-ray data obtained for **3** ($R_1$ = 0.1231) does not allow detailed information of bond lengths and angles. However, the X-ray structure of **3** (Figure 1) is good enough to indicate clearly that the reaction of *n*BuLi with dpp-bian (1:1 molar ratio) occurs with the transfer of the butyl group to the imino carbon atom C(2) of the dpp-bian ligand, thus making this carbon atom a chiral center.

Table 1. Selected bond lengths [Å] for **4**–**6**. M[a] = Li(2) for compound **4** and Ge for compound **6**.

| Compound | **4** | **5** | **6** |
|---|---|---|---|
| C(1)–N(1) | 1.285(3) | 1.274(3) | 1.286(3) |
| C(2)–N(2) | 1.485(3) | 1.497(3) | 1.468(3) |
| C(1)–C(2) | 1.561(3) | 1.542(3) | 1.533(3) |
| C(2)–C(37) | 1.561(4) | 1.535(3) | 1.558(3) |
| Li(1)–N(2) | 2.071(5) | | |
| M[a]–N(1) | 2.007(5) | | 2.1182(19) |
| M[a]–N(2) | 1.978(5) | | 1.8723(19) |
| Li(1a)–C(41) | 2.265(6) | | |
| Li(1)–C(41) | 2.321(6) | | |
| M[a]–C(41) | 2.087(6) | | |
| M[a]–Li(1) | 2.307(6) | | |
| Li(1)–Li(1a) | 2.562(10) | | |
| M[a]–Cl | | | 2.3500(7) |

Table 2. Selected bond angles [°] for **4**, **5** and **6**. M[a] = Li(2) for compound **4** and Ge for compound **6**.

| Compound | **4** | **5** | **6** |
|---|---|---|---|
| N(1)–C(1)–C(2) | 120.2(2) | 119.6(2) | 117.7(2) |
| N(2)–C(2)–C(1) | 112.5(2) | 103.41(17) | 105.22(18) |
| N(2)–C(2)–C(37) | 108.75(19) | 112.66(18) | 111.90(19) |
| C(1)–C(2)–C(37) | 106.2(2) | 112.19(18) | 110.28(18) |
| C(1)–N(1)–M[a] | 102.1(2) | | |
| C(2)–N(2)–M[a] | 101.9(2) | | |
| C(2)–N(2)–Li(1) | 130.9(2) | | |
| N(2)–Li(1)–C(41a) | 129.2(3) | | |
| N(2)–M[a]–N(1) | 93.5(2) | | 81.46(8) |
| N(2)–M[a]–C(41) | 111.2(2) | | |
| N(1)–M[a]–C(41) | 153.0(3) | | |
| N(1)–M[a]–Cl(1) | | | 93.06(5) |
| N(2)–M[a]–Cl(1) | | | 102.68(6) |

In the solid state, compound **4** (Figure 2) is the centrosymmetric dimer of the 1:1 adduct of solvent-free **3** with *n*BuLi. This dimer is formed by interaction of all four lithium atoms with the two $\mu_3$-bridging *n*Bu(Li) carbanions. Within the monomeric units, the bonding modes of the two lithium atoms relative to the [dpp-bian(*n*Bu)]$^-$ anion are different. Li(2) is connected with both N(1) and N(2) of the amido[N(2)]–imino[N(1)] ligand, while Li(1) is linked only to N(2). The amido–imino character of the alkylated dpp-bian ligand is manifested by the bond length within the N(1)–C(1)–C(2)–N(2) fragment. The length of the C(1)–N(1) bond [1.285(3) Å] is close to that of the C=N double

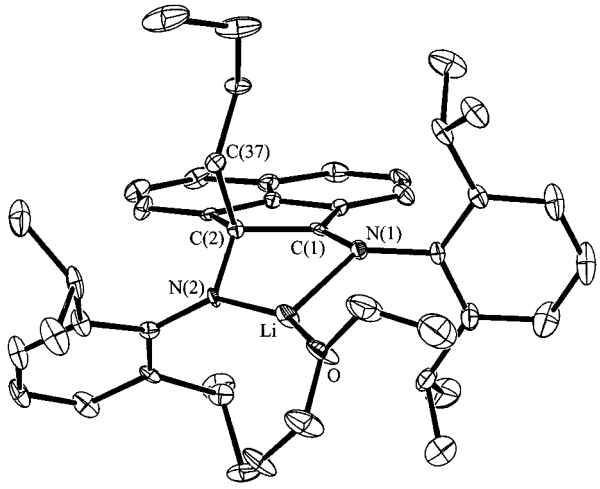


Figure 1. Molecular structure of **3**. Hydrogen atoms are omitted for clarity. Thermal ellipsoids are drawn at 30% probability.

bond in free dpp-bian [1.282(4) Å],[22] whereas the C(2)–N(2) distance [1.485(3) Å] corresponds well with the average value of carbon–nitrogen single bonds. In spite of the different functionality of the nitrogen atoms in the [dpp-bian(*n*Bu)]$^-$ anion, the N(1)–Li(2) and N(2)–Li(2) distances are very similar [2.007(5) and 1.978(5) Å, respectively]. The distance of the Li(1) atom to the amido atom N(2) is 2.071(5) Å. Both *n*-butyl carbanions act as $\mu_3$-bridges between Li(2) and the symmetry-equivalent Li(1) and Li(1a) atoms (symmetry operation: *–x*, *–y*, *–z*). The same bridging mode of *n*-butyl anions has been observed in [{(*n*BuLi)$_4$(TMEDA)}$_\infty$],[23] which exhibits a TMEDA-linked tetrameric cubane structure. The distances C(41)–Li(1) [2.321(6) Å] and C(41)–Li(1a) [2.265(6) Å], which are in the range of the Li–C distances in [{(*n*BuLi)$_4$(TMEDA)}$_\infty$], are significantly longer than the C(41)–Li(2) distance [2.087(6) Å].

The molecular structure of the metal-free amino-imine compound **5** (Figure 3) shows C–N distances that differ significantly, thus indicating an N(1)–C(1) double bond [1.274(3) Å] and an N(2)–C(2) single bond [1.497(3) Å]. The sum of the bond angles at N(2) (340°) points to a more tetrahedral (327°) than trigonal-planar (360°) arrangement.

The molecular structure of **6** (Figure 4) corresponds to a monomeric three-coordinate germylene. Because of the three different groups (chloride ion, amido- and imino-nitrogen atoms) bonded to the germanium atom and its lone electron-pair, the germanium atom is a chiral center. Taking into account that the C(2) atom in **6** is also chiral, one may expect the existence of two diastereomeric pairs of molecules, whereas in fact only one diastereomeric pair is present in the unit cell. In these two diastereomeric molecules the *n*Bu group and the chlorine atom are positioned at the same side of the plane formed by the metallacycle Ge–N(1)–C(1)–C(2)–N(2). Again, the difference between the amido and the imino functionality of the ligand is evident from the C–N distances [N(1)–C(1) = 1.286(3) and N(2)–C(2) = 1.468(3) Å]. However, in contrast to compound **4**,

  

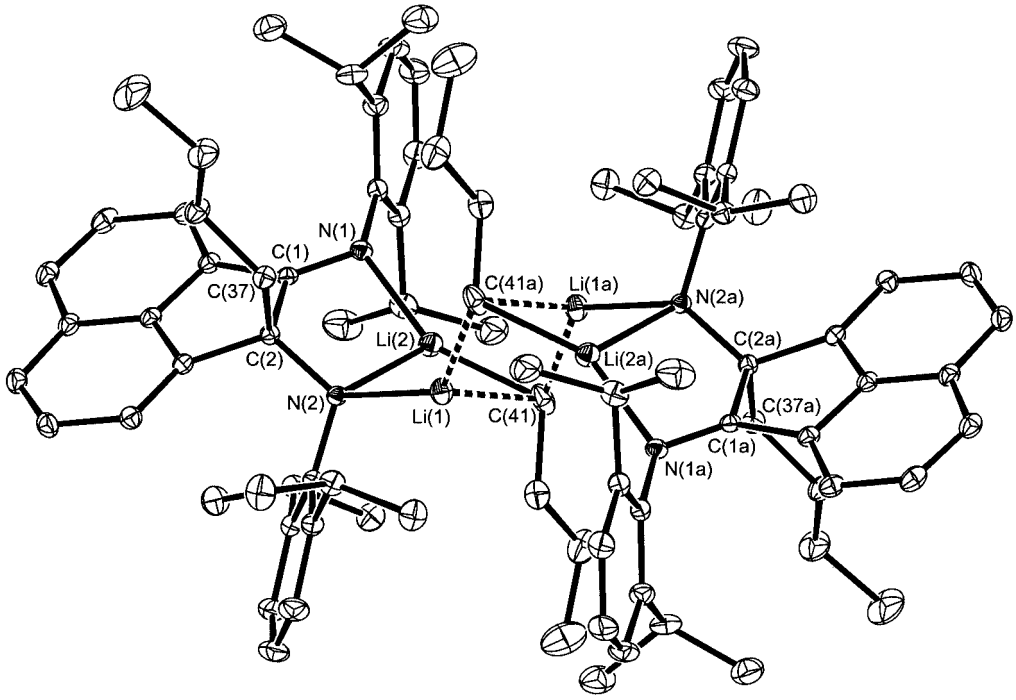


Figure 2. Molecular structure of **4**. Hydrogen atoms are omitted for clarity. Thermal ellipsoids are drawn at 30% probability.

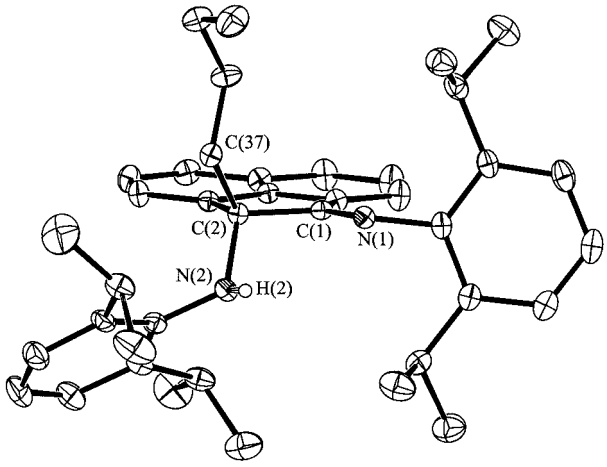


Figure 3. Molecular structure of **5**. Hydrogen atoms are omitted for clarity. Thermal ellipsoids are drawn at 30% probability.

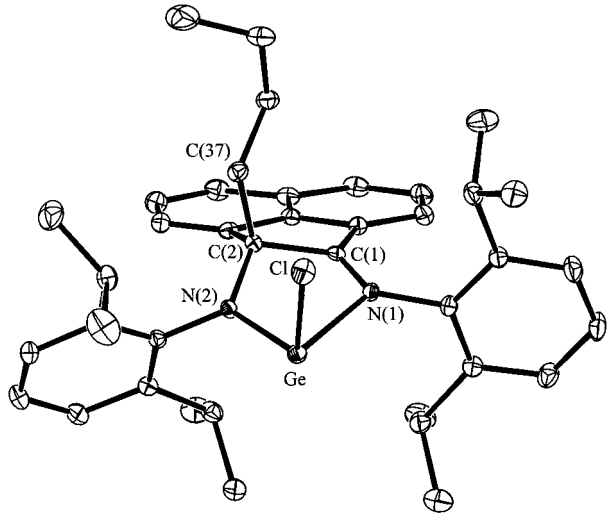


Figure 4. Molecular structure of **6**. Hydrogen atoms are omitted for clarity. Thermal ellipsoids are drawn at 30% probability.

there is also a pronounced difference in the length of the Ge–N(amido) bond [Ge–N(2) = 1.872(1) Å] and the Ge–N(imino) bond [Ge–N(1) = 2.118(1) Å]. The Ge–N(amido) distance compares well with the two Ge–N(amido) bonds in the germylene [(dpp-bian)Ge] [1.896(3) and 1.885(3) Å].[16] The Ge–Cl distance [2.3500(7) Å] is noticeably longer than the corresponding distance in the three-coordinate $Ge^{II}$ compound [(dpp-bian)GeCl] [2.2693(8) Å], which contains dpp-bian as a radical-anionic ligand.[17a] The sum of the bond angles (277.2°) at the germanium atom [81.46(8), 93.06(5), 102.68(6)°] is almost the same as in [(dpp-bian)GeCl] (276.8°).[17a]

## NMR Spectroscopy of 3–6

The addition of *n*BuLi to one of the C=N bonds of dpp-bian results in the formation of an asymmetric amido–imino structure, which, in turn, causes the inequivalence of all aromatic protons as well as of all methine protons of the isopropyl substituents (Figure 5).

The $^1$H NMR spectrum of a solution of the blue crystals of **3** in $C_6D_6$ contains twelve signals for the aromatic protons, ranging from $\delta$ = 7.48 to 6.53 ppm, and four signals for the methine protons at $\delta$ = 5.12, 3.44, 3.33, and

  

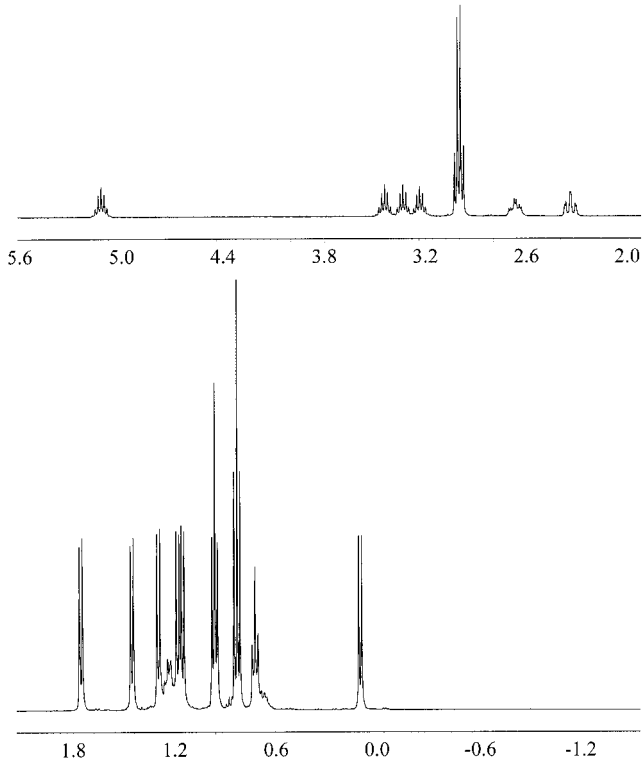


Figure 5. $^1$H NMR spectrum of **3** divided into two sections ($C_6D_6$, 400 MHz, 20 °C). The aromatic region is not shown.

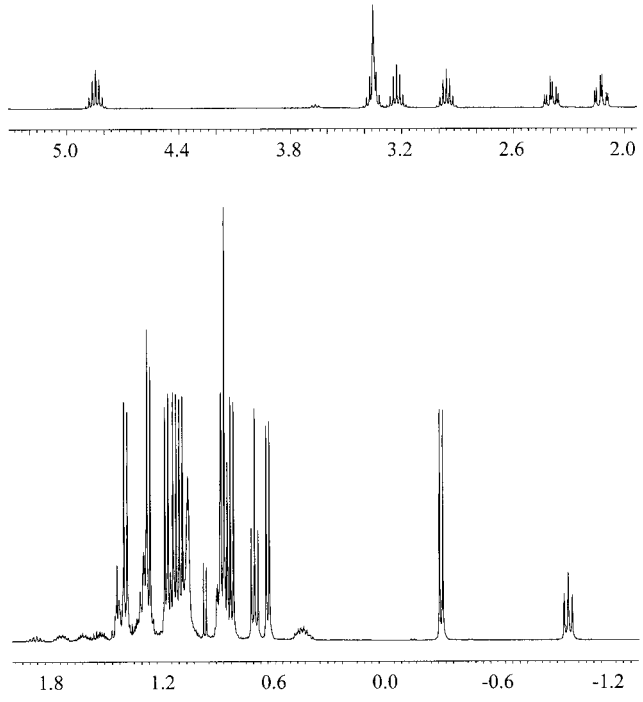


Figure 6. $^1$H NMR spectrum of **4** divided into two sections ([$D_{10}$]-$Et_2O$, 400 MHz, 20 °C). The aromatic region is not shown.

3.23 ppm (Figure 5a). Due to the restricted rotation around the N–C(*ipso*-Ph) bonds, all eight methyl groups become unequal and appear as eight doublets in the range from $\delta$ = 1.75 to 0.09 ppm (Figure 5b). The presence of the chiral carbon atom C(2) next to the methylene protons of the *n*Bu group causes the inequivalence of the α-$CH_2$(*n*Bu) protons and the appearance of two triplets of doublets at $\delta$ = 2.67 and 2.33 ppm. The $CH_3$(*n*Bu) group gives rise to a triplet at $\delta$ = 0.72 ppm, whereas the β- and γ-$CH_2$(*n*Bu) protons appear as multiplets at $\delta$ = 1.23 and 0.68 ppm. The signals of the coordinated $Et_2O$ molecule are centered at $\delta$ = 3.00 (q) and 0.83 (t) ppm. Dissolution of **3** in [$D_{10}$]$Et_2O$ does not cause significant changes in the $^1$H NMR spectrum. Thus, the four signals of the methine protons appear as septets at $\delta$ = 4.84, 3.35, 3.23 and 2.96 ppm, the nonequivalent α-$CH_2$(*n*Bu) protons give rise to two triplets of doublets at $\delta$ = 2.40 and 2.12 ppm, and the eight doublet signals for the unequal methyl groups are found between $\delta$ = 1.40 and –0.30 ppm.

The $^1$H NMR spectrum of **4** recorded in $C_6D_6$ (red solution) reveals only broadened signals, which could not be assigned. However, a simple $^1$H NMR spectrum (Figure 6) was obtained from a solution of compound **4** in [$D_{10}$]$Et_2O$ (blue solution) in which the positions of all signals of the amido–imino ligand are identical with those of the $^1$H NMR spectrum of solutions of compound **3** in [$D_{10}$]$Et_2O$.

Unexpectedly, the $^1$H NMR spectrum of compound **5** in [$D_8$]THF (Figure 7) shows signals for only eight of the twelve aromatic protons, and of the total of four methine protons belonging to the isopropyl substituents only two give distinguishable signals which are superimposed upon each other and centered at $\delta$ = 3.08 and 3.01 ppm (Figure 7). Also, only four of the eight doublet signals expected for the $CH_3$(*i*Pr) protons can be located. However, it should be noted that in the aromatic and aliphatic regions in which the missing signals would be expected, a visible raising of the baseline is observed. We attribute this to a significant broadening of those signals due to a slow (on the NMR timescale) dynamic process within the molecules of **5** in solution and suggest an umbrella-like inversion at the amino nitrogen atom N(2). Such a process affects all the protons of the 2,6-*i*$Pr_2$Ph ring bonded to N(2) and leads to a broadening of the $^1$H resonances of this substituent. In contrast, the signal of the proton connected directly to N(2)

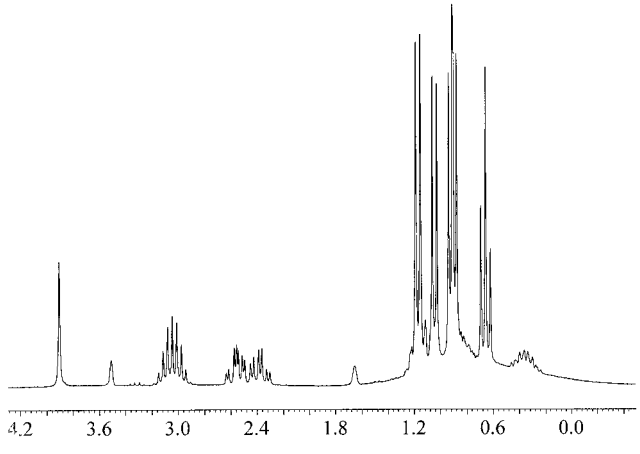


Figure 7. $^1$H NMR spectrum of **5** ([$D_8$]THF, 200 MHz, 20 °C). The aromatic region is not shown.

  

appears as a sharp singlet at $\delta$ = 3.91 ppm. The α-$CH_2$(*n*Bu) protons give rise to two triplets of doublets at $\delta$ = 2.56 and 2.38 ppm and the $CH_3$(*n*Bu) signal appears as a triplet at $\delta$ = 0.66 ppm.

The $^1$H NMR spectrum of compound **6** in [$D_8$]THF shows analogous signal sets to the $^1$H NMR spectrum of compound **3** recorded in [$D_{10}$]$Et_2O$, which differ only with respect to the chemical shifts of the signals. Nevertheless, the spectrum has one noticeable feature. In the $^1$H NMR spectrum of **6**, the α-$CH_2$(*n*Bu) protons appear at $\delta$ = 3.90 and 2.41 (2 td) ppm, thus displaying a much larger diastereotopic splitting constant (1.49 Hz) than those observed in the spectra of **3** (0.28 Hz in $Et_2O$), **4** (0.28 Hz in $Et_2O$), and **5** (0.18 Hz in THF). We believe that the high value of the splitting constant of **6** is caused by the chirality at the germanium atom.

## Conclusions

We have been able to demonstrate that the addition of *n*BuLi to one C=N bond of dpp-bian produces a new, asymmetrically chelating amido–imino ligand system which is expected to be useful for the preparation of new metal-based reagents for organic synthesis.

## Experimental Section

**General Remarks:** All manipulations were carried out under nitrogen using standard Schlenk techniques. Hexane, diethyl ether, and benzene were dried by distillation from sodium/benzophenone. *n*BuLi (2.5 M in hexane) was purchased from ACROS. The deuterated solvents [$D_8$]THF (Aldrich), $C_6D_6$ (Aldrich), and [$D_{10}$]$Et_2O$ (Euriso-top) used for NMR experiments were dried with sodium/benzophenone at ambient temperature and, just prior to use, were condensed under vacuum into the NMR tubes already containing the respective compound. Melting points were measured in sealed capillaries. IR spectra were recorded with an FTIR FSM-1201 spectrometer (Monitoring Ltd.), and $^1$H NMR spectra were obtained with Bruker DPX-200 and Bruker DRX-400 NMR spectrometers.

**[{dpp-bian(*n*Bu)}Li($Et_2O$)] (3):** Addition of 0.8 mL of *n*BuLi (2.5 M in hexane; 2.0 mmol) to a stirred suspension of dpp-bian (1.0 g, 2.0 mmol) in $Et_2O$ (20 mL) at room temperature caused immediate dissolution of dpp-bian and formation of a clear blue-green solution. The foamy residue left after evaporation of the solvent was recrystallized from hexane. The thin blue plates of compound **3** formed within 20 h were collected by decantation of the mother liquor. Yield: 0.56 g (44%); m.p. > 120 °C (dec.). $C_{44}H_{59}LiN_2O$ (638.91): calcd. C 82.72, H 9.31; found C 82.59, H 9.17. $^1$H NMR (400 MHz, $C_6D_6$, 20 °C): $\delta$ = 7.48 (dd, *J* = 7.6 and 1.7 Hz, 1 H, CH arom.), 7.42 (d, *J* = 8.0 Hz, 1 H, CH arom.), 7.29 (d, *J* = 8.0 Hz, 1 H, CH arom.), 7.26 (dd, *J* = 7.6 and 1.7 Hz, 1 H, CH arom.), 7.26 (pseudo t, *J* = 7.6 Hz, 1 H, CH arom.), 7.24 (d, *J* = 6.8 Hz, 1 H, CH arom.), 7.18 (pseudo t, *J* = 7.6 Hz, 1 H, CH arom.), 7.10 (dd, *J* = 7.6 and 1.7 Hz, 1 H, CH arom.), 7.08 (pseudo t, *J* = 7.2 Hz, 1 H, CH arom.), 6.87 (pseudo t, *J* = 7.8 Hz, 1 H, CH arom.), 6.58 (d, *J* = 7.2 Hz, 1 H, CH arom.), 6.53 (d, *J* = 6.8 Hz, 1 H, CH arom.), 5.12 [pseudo t, *J* = 6.8 Hz, 1 H, C*H*-$(CH_3)_2$], 3.44 [pseudo t, *J* = 6.8 Hz, 1 H, C*H*$(CH_3)_2$], 3.33 [pseudo t, *J* = 6.8 Hz, 1 H, C*H*$(CH_3)_2$], 3.23 [pseudo t, *J* = 6.8 Hz, 1 H, C*H*$(CH_3)_2$], 3.00 (q, *J* = 7.0 Hz, 4 H, $Et_2O$), 2.67 (td, *J* = 12.5 and 4.2 Hz, 1 H, CH*H*$(CH_2)_2CH_3$], 2.33 [td, *J* = 12.5 and 4.2 Hz, 1 H, C*H*H$(CH_2)_2CH_3$], 1.75 [d, *J* = 6.8 Hz, 3 H, CH(C*H*$_3)_2$], 1.45 [d, *J* = 6.8 Hz, 3 H, CH(C*H*$_3)_2$], 1.30 [d, *J* = 6.8 Hz, 3 H, CH(C*H*$_3)_2$], 1.18 [d, *J* = 6.8 Hz, 3 H, CH(C*H*$_3)_2$], 1.15 [d, *J* = 6.8 Hz, 3 H, CH(C*H*$_3)_2$], 0.97 [d, *J* = 6.8 Hz, 3 H, CH(C*H*$_3)_2$], 0.95 [d, *J* = 6.8 Hz, 3 H, CH(C*H*$_3)_2$], 0.83 (t, *J* = 7.0 Hz, 6 H, $Et_2O$), 0.72 [t, *J* = 7.0 Hz, 3 H, $(CH_2)_3CH_3$], 0.10 [d, *J* = 6.8 Hz, 3 H, CH(C*H*$_3)_2$] ppm.

**[{dpp-bian(*n*Bu)Li}*n*BuLi]$_2$ (4):** Addition of 1.8 mL of *n*BuLi (2.5 M in hexane; 4.4 mmol) to a stirred suspension of dpp-bian (1.0 g, 2.0 mmol) in hexane (20 mL) at room temperature caused dissolution of dpp-bian and precipitation of a red crystalline product. The product was filtered off and recrystallized from hexane (35 mL) to yield 1.08 g (81%) of compound **4** as red crystals. M.p. > 130 °C darkening, >181 °C melting (dec.). $C_{88}H_{116}Li_4N_4{\cdot}C_6H_{14}$ (1343.8): calcd. C 84.01, H, 9.75; found C 83.13, H, 9.21. $^1$H NMR (400 MHz, $Et_2O$, 20 °C): $\delta$ = 7.74 (d, *J* = 8.2 Hz, 1 H, CH arom.), 7.45 (d, *J* = 8.2 Hz, 1 H, CH arom.), 7.30 (m, 1 H, CH arom.), 7.25 (m, 2 H, CH arom.), 7.16 (pseudo t, *J* = 8.2 Hz, 1 H, CH arom.), 7.12 (pseudo t, *J* = 8.2 Hz, 1 H, CH arom.), 7.02 (dd, *J* = 7.3 and 1.9 Hz, 1 H, CH arom.), 6.68 (pseudo t, *J* = 7.3 Hz, 1 H, CH arom.), 6.61 (dd, *J* = 7.3 and 1.9 Hz, 1 H, CH arom.), 6.38 (d, *J* = 7.3 Hz, 1 H, CH arom.), 6.11 (d, *J* = 6.9 Hz, 1 H, CH arom.), 4.84 [pseudo t, *J* = 6.9 Hz, 1 H, C*H*$(CH_3)_2$], 3.35 [pseudo t, *J* = 6.9 Hz, 1 H, C*H*$(CH_3)_2$], 3.23 [pseudo t, *J* = 6.9 Hz, 1 H, C*H*-$(CH_3)_2$], 2.96 [pseudo t, *J* = 6.9 Hz, 1 H, C*H*$(CH_3)_2$], 2.40 [td, *J* = 12.7 and 4.7 Hz, 1 H, CH*H*$(CH_2)_2CH_3$], 2.12 [td, *J* = 12.7 and 3.5 Hz, 1 H, C*H*H$(CH_2)_2CH_3$], 1.40 [d, *J* = 6.9 Hz, 3 H, CH-(C*H*$_3)_2$], 1.28 [d, *J* = 6.9 Hz, 3 H, CH(C*H*$_3)_2$], 1.18 [d, *J* = 6.9 Hz, 3 H, CH(C*H*$_3)_2$], 1.14 [d, *J* = 6.9 Hz, 3 H, CH(C*H*$_3)_2$], 1.11 [d, *J* = 6.9 Hz, 3 H, CH(C*H*$_3)_2$], 0.87 [m, 8 H, $LiCH_2(CH_2)_2CH_3$], 0.83 [d, *J* = 6.9 Hz, 3 H, CH(C*H*$_3)_2$], 0.71 [t, *J* = 7.2 Hz, 3 H, $(CH_2)_3CH_3$], 0.64 [d, *J* = 6.9 Hz, 3 H, CH(C*H*$_3)_2$], –0.30 [d, *J* = 6.9 Hz, 3 H, CH(C*H*$_3)_2$], –0.98 [t, *J* = 7.0 Hz, 3 H, $LiCH_2$-$(CH_2)_2CH_3$] ppm.

**(dpp-bian)(H)(*n*Bu) (5):** Addition of $H_2O$ (0.3 mL) to a solution of **3** [prepared in situ from 1.0 g (2.0 mmol) of dpp-bian in $Et_2O$] caused an immediate yellow coloring of the reaction mixture. After evaporation of the solvent under reduced pressure, the residue was dried in vacuo for 1 h and was then recrystallized from $Et_2O$ (20 mL) to yield 0.85 g (76%) of compound **5** as yellow drusy crystals; m.p. > 179 °C. $C_{40}H_{50}N_2$ (558.82): calcd. C 85.97, H, 9.02; found C 85.88, H 8.98. IR (Nujol): $\tilde{\nu}$ = 3359 (w), 3057 (w), 1663 (vs), 1621 (w), 1598 (w), 1582 (m), 1491 (w), 1379 (s), 1363 (s), 1328 (m), 1305 (w), 1269 (w), 1252 (m), 1193 (m), 1179 (w), 1143 (w), 1113 (m), 1098 (w), 1051 (w), 1035 (m), 1019 (w), 1003 (w), 957 (w), 935 (m), 907 (w), 890 (w), 830 (s), 808 (w), 798 (s), 785 (vs), 769 (s), 755 (s), 726 (m), 708 (m), 667 (w), 649 (w), 632 (w), 606 (w), 597 (w), 559 (w), 538 (w), 522 (w), 511 (w), 469 (w), 449 (w) cm$^{-1}$. $^1$H NMR (200 MHz, [$D_8$]THF, 20 °C): $\delta$ = 7.48 (d, *J* = 8.3 Hz, 1 H, CH arom.), 6.64 (d, *J* = 8.3 Hz, 1 H, CH arom.), 7.28–7.12 (m, 4 H, CH arom.), 6.51 (d, *J* = 7.3 Hz, 1 H, CH arom.), 6.35 (d, *J* = 7.0 Hz, 1 H, CH arom.), 3.91 (s, 1 H, N–H), 3.08 [pseudo t, *J* = 6.8 Hz, 1 H, C*H*$(CH_3)_2$], 3.01 [pseudo t, *J* = 6.8 Hz, 1 H, C*H*$(CH_3)_2$], 2.56 (td, *J* = 12.2 and 3.8 Hz, 1 H, CH*H*$(CH_2)_2$-$CH_3$], 2.38 [td, *J* = 12.2 and 5.0 Hz, 1 H, C*H*H$(CH_2)_2CH_3$], 1.17 [d, *J* = 6.8 Hz, 3 H, CH(C*H*$_3)_2$], 1.05 [d, *J* = 6.8 Hz, 3 H, CH-(C*H*$_3)_2$], 0.92 [d, *J* = 6.8 Hz, 3 H, CH(C*H*$_3)_2$], 0.89 [d, *J* = 6.8 Hz, 3 H, CH(C*H*$_3)_2$], 0.66 [t, *J* = 7.3 Hz, 6 H, $(CH_2)_3CH_3$] ppm.

  

**[{dpp-bian(*n*Bu)}GeCl] (6):** Addition of a solution of **3** [prepared in situ from 1.0 g (2.0 mmol) of dpp-bian in $Et_2O$] to a stirred suspension of $GeCl_2$(dioxane) (0.46 g, 2.0 mmol) in $Et_2O$ (10 mL) caused a change of the color of the solution from blue to brown. The solution should be filtered immediately after mixing the reagents, otherwise **6** starts to crystallize from the reaction mixture on standing. Slow evaporation of the solvent from the filtrate at low pressure caused the crystallization of **6** as red crystals. Yield: 1.18 g (89%); m.p. 238 °C. $C_{40}H_{49}ClGeN_2$ (665.85): calcd. C 72.15, H 7.42; found C 72.05, H 7.30. IR (Nujol): $\tilde{\nu}$ = 1624 (s), 1589 (s), 1491 (w), 1378 (s), 1364 (w), 1315 (m), 1249 (s), 1221 (w), 1203 (m), 1187 (m), 1162 (w), 1141 (w), 1109 (m), 1099 (m), 1060 (m), 1050 (w), 1035 (m), 1005 (w), 961 (w), 933 (w), 919 (m), 884 (w), 861 (m), 833 (s), 819 (w), 800 (s), 784 (vs), 768 (w), 760 (s), 748 (m), 723 (s), 700 (w), 676 (w), 653 (w), 635 (w), 618 (m), 599 (w), 582 (w), 546 (w), 527 (w), 516 (w), 499 (w), 480 (m), 465 (w), 451 (w), 442 (w), 419 (m), 403 (m) $cm^{-1}$. $^1H$ NMR (200 MHz, [$D_8$]THF, 20 °C): $\delta$ = 8.08 (d, $J$ = 8.3 Hz, 1 H, CH arom.), 7.77 (d, $J$ = 8.3 Hz, 1 H, CH arom.), 7.54–7.31 (m, 6 H, CH arom.), 7.22 (pseudo t, $J$ = 7.3 Hz, 1 H, CH arom.), 6.97 (dd, $J$ = 7.5 and 1.7 Hz, 1 H, CH arom.), 6.55 (d, $J$ = 7.3 Hz, 1 H, CH arom.), 6.15 (d, $J$ = 7.0 Hz, 1 H, CH arom.), 4.66 [pseudo t, $J$ = 6.8 Hz, 1 H, C*H*-$(CH_3)_2$], 3.90 [td, $J$ = 13.0 and 4.0 Hz, 1 H, CH*H*$(CH_2)_2CH_3$], 3.79 [pseudo t, $J$ = 6.8 Hz, 1 H, C*H*$(CH_3)_2$], 3.01 [pseudo t, $J$ = 6.8 Hz, 1 H, C*H*$(CH_3)_2$], 2.61 [pseudo t, $J$ = 6.8 Hz, 1 H, C*H*$(CH_3)_2$], 2.41 [td, $J$ = 13.0 and 4.5 Hz, 1 H, C*H*H$(CH_2)_2CH_3$], 1.45 [d, $J$ = 6.9 Hz, 3 H, CH(C$H_3$)$_2$], 1.42 [d, $J$ = 6.9 Hz, 3 H, CH(C$H_3$)$_2$], 1.24 [d, $J$ = 6.9 Hz, 3 H, CH(C$H_3$)$_2$], 1.23 [d, $J$ = 6.9 Hz, 3 H, CH-(C$H_3$)$_2$], 1.20 [d, $J$ = 6.9 Hz, 3 H, CH(C$H_3$)$_2$], 1.13 [m, 3 H, $CH_2$(C$H_2$)$_2$C$H_3$], –0.06 [m, 1 H, $CH_2$(C$H_2$)$_2$C$H_3$], 0.90 [d, $J$ = 6.9 Hz, 3 H, CH(C$H_3$)$_2$], 0.66 [t, $J$ = 7.2 Hz, 3 H, $(CH_2)_3$C$H_3$], 0.64 [d, $J$ = 6.9 Hz, 3 H, CH(C$H_3$)$_2$], 0.05 [d, $J$ = 6.9 Hz, 3 H, CH-(C$H_3$)$_2$] ppm.

**Single-Crystal X-ray Structure Determination of 4–6:** The data were collected with a Siemens SMART CCD diffractometer (graphite-monochromated Mo-$K_\alpha$ radiation, $\omega$-scan technique, $\lambda$ = 0.71073 Å) at 173 K. **4:** $C_{88}H_{116}Li_4N_4{\cdot}C_6H_{14}$, $M$ = 1343.78, monoclinic, $a$ = 31.9219(11), $b$ = 12.7641(5), $c$ = 22.8212(8) Å, $\beta$ = 113.4070(10)°, $V$ = 8533.4(5) Å$^3$, $T$ = 173(2) K, space group $C2/c$, $Z$ = 4, $\mu$ = 0.059 $mm^{-1}$, 26677 reflections measured, 7521 unique ($R_{int}$ = 0.0895) which were used in all calculations. $R_1$ [$I > 2\sigma(I)$] = 0.0694, w$R_1$ (all data) = 0.1201. **5:** $C_{40}H_{50}N_2$, $M$ = 558.82, monoclinic, $a$ = 19.0920(8), $b$ = 9.1708(4), $c$ = 19.2750(7) Å, $\beta$ = 90.164(1)°, $V$ = 3374.8(2) Å$^3$, $T$ = 173(2) K, space group $P2_1/c$, $Z$ = 4, $\mu$ = 0.063 $mm^{-1}$, 20271 reflections measured, 5929 unique ($R_{int}$ = 0.1428) which were used in all calculations. $R_1$ [$I > 2\sigma(I)$] = 0.0593, w$R_1$ (all data) = 0.1240. **6:** $C_{40}H_{49}ClGeN_2$, $M$ = 665.85, monoclinic, $a$ = 9.7607(3), $b$ = 17.3631(6), $c$ = 21.0357(7) Å, $\beta$ = 97.9650(10)°, $V$ = 3530.7(2) Å$^3$, $T$ = 173(2) K, space group $P2_1/n$, $Z$ = 4, $\mu$ = 0.973 $mm^{-1}$, 23727 reflections measured, 6922 unique ($R_{int}$ = 0.0747) which were used in all calculations. $R_1$ [$I > 2\sigma(I)$] = 0.0409, w$R_1$ (all data) = 0.0940. The structures were solved by direct methods using SHELXS-97[24] and were refined on $F^2$ using SHELXL-97.[25] All non-hydrogen atoms were refined anisotropically and the hydrogen atoms were placed in calculated positions and assigned to an isotropic displacement parameter of 0.08 Å$^2$. SADABS[26] was used to perform area-detector scaling and absorption corrections. The geometrical aspects of the structures were analyzed with the PLATON program.[27] CCDC-605326 (**4**), -605327 (**5**), and -605328 (**6**) contain the supplementary crystallographic data for this paper. These data can be obtained free of charge from The Cambridge Crystallographic Data Centre via www.ccdc.cam.ac.uk/data_request/cif.

## Acknowledgments

This work was supported by the Russian Foundation for Basic Research (grant no. 05-03-32643), the Russian Science and Innovation Agency (grant no. 2006-RI-19.0/001/206) (I. F.) as well as the Fonds der Chemischen Industrie and the Deutsche Forschungsgemeinschaft (H. S.).

[1] a) M. W. van Laren, C. J. Elsevier, *Angew. Chem. Int. Ed.* **1999**, *38*, 3715; b) A. M. Kluwer, T. S. Koblenz, T. Jonischkeit, K. Woelk, C. J. Elsevier, *J. Am. Chem. Soc.* **2005**, *127*, 15470.
[2] a) R. van Belzen, H. Hoffmann, C. J. Elsevier, *Angew. Chem. Int. Ed. Engl.* **1997**, *36*, 1743; b) G. A. Grasa, R. Singh, E. D. Stevens, S. P. Nolan, *J. Organomet. Chem.* **2003**, *687*, 269.
[3] A. Heumann, L. Giordano, A. Tenaglia, *Tetrahedron Lett.* **2003**, *44*, 1515.
[4] J. W. Sprengers, M. de Greef, M. A. Duin, C. J. Elsevier, *Eur. J. Inorg. Chem.* **2003**, 3811.
[5] a) E. Cherian, E. B. Lobkovsky, G. W. Coates, *Chem. Commun.* **2003**, *20*, 2566; b) F. Al-Abaidi, Z. Ye, S. Zhu, *Macromol. Chem. Phys.* **2003**, *204*, 1653; c) V. Fassina, C. Ramminger, M. Seferin, R. S. Mauler, R. F. de Souza, A. L. Monteiro, *Macromol. Rapid Commun.* **2003**, *24*, 667; d) M. D. Leatherman, S. A. Svejda, L. K. Johnson, M. Brookhart, *J. Am. Chem. Soc.* **2003**, *125*, 3068; e) A. E. Cherian, J. M. Rose, E. B. Lobkovsky, G. W. Coates, *J. Am. Chem. Soc.* **2005**, *127*, 13770; f) D. H. Camacho, E. V. Salo, Z. Guan, J. W. Ziller, *Organometallics* **2005**, *24*, 4933; g) S. S. Ivanchev, V. K. Badaev, N. I. Ivancheva, E. V. Sviridova, S. Ya. Khaikin, D. G. Rogozin, A. S. Abakunchik, *Vysokomol. Soedin., Ser. A Ser. B* **2005**, *47*, 934.
[6] I. Kim, J.-M. Hwang, J. K. Lee, C. S. Ha, S. I. Woo, *Macromol. Rapid Commun.* **2003**, *24*, 508.
[7] D. Takeuchi, A. Yasuda, K. Osakada, *Dalton Trans.* **2003**, 2029.
[8] D. Takeuchi, K. Anada, K. Osakada, *Bull. Chem. Soc. Jpn.* **2005**, *78*, 1868.
[9] J. Kiesewetter, W. Kaminsky, *Chem. Eur. J.* **2003**, *9*, 1750.
[10] B. Binotti, C. Carfagna, C. Zuccaccia, A. Macchioni, *Chem. Commun.* **2005**, 92.
[11] a) B. S. Williams, M. D. Leatherman, P. S. White, M. Brookhart, *J. Am. Chem. Soc.* **2005**, *127*, 5132; b) J. Merna, J. Cihlar, M. Kucera, A. Deffieux, H. Cramail, *Eur. Polym. J.* **2005**, *41*, 303; c) W. Liu, M. Brookhart, *Organometallics* **2004**, *23*, 6099; d) D. H. Camacho, E. V. Salo, J. W. Ziller, Z. Guan, *Angew. Chem. Int. Ed.* **2004**, *43*, 1821.
[12] a) I. L. Fedushkin, A. A. Skatova, V. A. Chudakova, G. K. Fukin, *Angew. Chem. Int. Ed.* **2003**, *42*, 3294; b) I. L. Fedushkin, A. A. Skatova, V. A. Chudakova, V. K. Cherkasov, G. K. Fukin, M. A. Lopatin, *Eur. J. Inorg. Chem.* **2004**, 388.
[13] I. L. Fedushkin, A. A. Skatova, V. A. Chudakova, G. K. Fukin, S. Dechert, H. Schumann, *Eur. J. Inorg. Chem.* **2003**, 3336.
[14] A. N. Lukoyanov, I. L. Fedushkin, M. Hummert, H. Schumann, *Russ. Chem. Bull.*, in press.
[15] a) H. Schumann, M. Hummert, A. N. Lukoyanov, I. L. Fedushkin, *Organometallics* **2005**, *24*, 3891; b) A. N. Lukoyanov, I. L. Fedushkin, M. Hummert, H. Schumann, *Z. Anorg. Allg. Chem.*, in press.
[16] I. L. Fedushkin, A. A. Skatova, V. A. Chudakova, N. M. Khvoinova, A. Yu. Baurin, S. Dechert, M. Hummert, H. Schumann, *Organometallics* **2004**, *23*, 3714.
[17] a) I. L. Fedushkin, N. M. Khvoinova, A. Yu. Baurin, G. K. Fukin, V. K. Cherkasov, M. P. Bubnov, *Inorg. Chem.* **2004**, *43*, 7807; b) I. L. Fedushkin, N. M. Khvoinova, A. Yu. Baurin, V. A. Chudakova, A. A. Skatova, V. K. Cherkasov, G. K. Fukin, E. V. Baranov, *Russ. Chem. Bull.* **2006**, *55*, 74.
[18] I. L. Fedushkin, A. A. Skatova, M. Hummert, H. Schumann, *Eur. J. Inorg. Chem.* **2005**, 1601.

  

[19] I. L. Fedushkin, A. A. Skatova, V. K. Cherkasov, V. A. Chudakova, S. Dechert, M. Hummert, H. Schumann, *Chem. Eur. J.* **2003**, *9*, 5778.
[20] I. L. Fedushkin, V. M. Makarov, E. C. E. Rosenthal, G. K. Fukin, *Eur. J. Inorg. Chem.* **2006**, 827.
[21] a) I. L. Fedushkin, N. M. Khvoinova, A. A. Skatova, G. K. Fukin, *Angew. Chem. Int. Ed.* **2003**, *42*, 5223; b) I. L. Fedushkin, A. G. Morozov, O. V. Rassadin, G. K. Fukin, *Chem. Eur. J.* **2005**, *11*, 5749; c) I. L. Fedushkin, A. A. Skatova, G. K. Fukin, M. Hummert, H. Schumann, *Eur. J. Inorg. Chem.* **2005**, 2332.
[22] I. L. Fedushkin, V. A. Chudakova, G. K. Fukin, S. Dechert, M. Hummert, H. Schumann, *Russ. Chem. Bull.* **2004**, *53*, 2744.
[23] N. D. R. Barnett, R. E. Mulvey, W. Clegg, P. A. O'Neil, *J. Am. Chem. Soc.* **1993**, *115*, 1573.
[24] G. M. Sheldrick, *SHELXS-97, Program for the Solution of Crystal Structures*, University of Göttingen, **1990**.
[25] G. M. Sheldrick, *SHELXL-97, Program for the Refinement of Crystal Structures*, University of Göttingen, **1997**.
[26] G. M. Sheldrick, *SADABS, Program for Empirical Absorption Correction of Area Detector Data*, University of Göttingen, **1996**.
[27] A. L. Spek, *PLATON, A Multipurpose Crystallographic Tool*, Utrecht University, **2000**.

Received: March 27, 2006
Published Online: June 29, 2006

  